

# Spin Squeezing of Atomic Ensembles via Nuclear-Electronic Spin Entanglement

T. Fernholz, H. Krauter, K. Jensen, J. F. Sherson,\* A. S. Sørensen, and E. S. Polzik†

*QUANTOP, Danish National Research Foundation Center for Quantum Optics,*

*Niels Bohr Institute, Copenhagen University, DK 2100, Denmark*

(Dated: June 1, 2018)

Entangled many body systems have recently attracted significant attention in various contexts. Among them, spin squeezed atoms and ions have raised interest in the field of precision measurements, as they allow to overcome quantum noise of uncorrelated particles [1, 2, 3, 4, 5, 6]. Precise quantum state engineering is also required as a resource for quantum computation, and spin squeezing can be used to create multi-partite entangled states [7]. Two-mode spin squeezed systems [8] have been used for elementary quantum communication protocols [9, 10]. Until now spin squeezing has been always achieved via generation of entanglement between different atoms of the ensemble [11, 12, 13]. In this Letter, we demonstrate for the first time ensemble spin squeezing generated by engineering the quantum state of each individual atom. More specifically, we entangle the nuclear and electronic spins of  $10^{12}$  Cesium atoms at room temperature. We verify entanglement and ensemble spin squeezing by performing quantum tomography on the atomic state.

Ensembles of neutral atoms in the form of cold gases as well as room-temperature vapor have emerged as important systems for the generation of entanglement and for the storage of quantum information [9, 10, 14, 15, 16, 17, 18, 19, 20]. It has been shown that ensemble spin squeezing can be used to significantly improve the fidelity of some existing quantum memory protocols [9]. In the majority of the work on ensemble entanglement alkali atoms used as memory units were treated as spin-1/2 systems, while their actual much higher total angular momenta were considered an unfortunate complication. Entanglement in those experiments could therefore be generated only between different atoms of the ensemble. In this Letter, we generate entanglement in an ensemble of spin-4 atoms by using their internal structure to squeeze the individual spins. Indeed, we can show that spin squeezing within the Cesium  $F = 4$  manifold is a signature of entanglement between the electron and the nucleus. However, as discussed below, the ensemble spin squeezing does not necessarily follow from the single atom spin squeezing. Therefore, we verify the collective squeezing by measurement of the collective spin state via strong coupling to off-resonant light. In particular, we perform for the first time quantum tomography of a non-classical state of an atomic ensemble.

We first consider a collection of ground state atoms, each prepared in the magnetic sublevel  $|F = 4, m_F = 4\rangle$  with respect to the  $x$  quantization axis. This fully stretched state is a product state, where both the nuclear and the electronic spin are in Eigenstates of their angular momentum projection operators with maximal Eigenvalues  $I_x = 7/2$  and  $S_x = 1/2$ , respectively. In the following, we denote the total spin operator of the ensemble  $\hat{\mathbf{J}}$ . For large atom numbers  $N$ , the total spin becomes macroscopic with  $\langle \hat{\mathbf{J}} \rangle = (J, 0, 0)$  in cartesian coordinates, and  $J = \hbar NF$ . The commutation relation  $[\hat{J}_y, \hat{J}_z] = i\hbar\hat{J}_x$  imposes an uncertainty relation, and the fully pumped ensemble is in a minimal uncertainty state with  $(\Delta\hat{J}_y)^2 = (\Delta\hat{J}_z)^2 = \hbar J/2$ . Such states are called coherent spin states (CSS) and set the standard quantum limit (SQL) to spin projection measurements. For a squeezed spin state (SSS), one of the orthogonal projections exhibits an uncertainty below the SQL. For useful spin squeezing, however, it is not sufficient to reduce the uncertainty below its initial value ( $\chi^2 = 2(\Delta\hat{J}_\perp)^2/\hbar J < 1$ ), but to compare it to a CSS with the same mean spin ( $\zeta^2 = 2(\Delta\hat{J}_\perp)^2/\hbar\langle|\hat{\mathbf{J}}|\rangle < 1$ ) [1, 21], or even more rigorously to the initial uncertainty in spin angle ( $\xi^2 = 2J(\Delta\hat{J}_\perp)^2/\hbar\langle|\hat{\mathbf{J}}|\rangle^2 < 1$ ) [22, 23]. The last condition is the strongest and provides a sufficient condition for entanglement of elementary spin-1/2 constituents [24]. It has to be met to improve quantum metrology with a given number of atoms, e.g., the precision of atomic clocks.

Unconditional spin squeezing can be achieved by applying a Hamiltonian that depends non-linearly on cartesian spin components orthogonal to the mean spin [21]. A Hamiltonian of the form  $\hat{H}_s = \alpha\hat{F}_z^2$  acting on a spin  $\hat{\mathbf{F}}$  induces a process called one-axis twisting. Starting from a CSS aligned along the  $x$ -direction, the spin is rotated about the  $z$ -axis in proportion to its fluctuating  $z$ -component. The initially symmetric quasi-probability distribution (QPD) will be sheared and appear squeezed in the  $y, z$  plane in a slightly rotated basis  $\hat{F}_{y'}, \hat{F}_{z'}$ . At the same time, the magnitude of the mean spin is reduced as the QPD bends around the spherical phase space for constant  $F$ .

In our experiment we generate a squeezing Hamiltonian using the tensor light shift induced by an off-resonant light field. In case of linear polarization along the  $z$ -direction with classical field amplitude  $E_z$ , the interaction with an atomic spin  $\hat{\mathbf{F}}$  reduces to an atomic

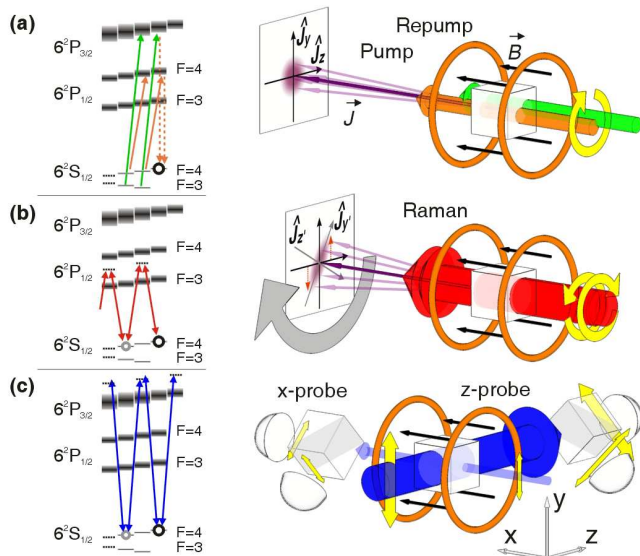


FIG. 1: Pulse sequence and level scheme for atomic state preparation and quantum state reconstruction. (a) Optical pumping creates a macroscopic spin  $\vec{J}$  in a CSS, aligned with the magnetic field  $\vec{B}$ . (b) A Raman transition creates a coherent superposition of even magnetic sublevels, which shears the QPD in the rotating frame and decreases the mean spin. (c) The squeezed spin state of the ensemble is characterized via off-resonant Faraday interaction with a probe beam, propagating in the  $z$ -direction. Quantum noise limited polarization measurements reveal the statistics of the atomic angular momentum projections  $\hat{J}_{y'}$  and  $\hat{J}_{z'}$ , which are precessing about the  $x$ -axis. Simultaneously, a weak measurement along the  $x$ -axis determines the magnitude of the mean atomic spin  $\langle \hat{J}_x \rangle$ . See methods section for details.

Hamiltonian of the form:

$$H_s = -\frac{1}{4}(\alpha_0 |E_z|^2 + \alpha_2 |E_z|^2 \hat{F}_z^2). \quad (1)$$

While the scalar polarizability  $\alpha_0$  simply results in an overall Stark shift, its tensor part, proportional to  $\alpha_2$ , provides the basis for spin squeezing.

In the  $x$ -basis, the  $z$ -polarized field can be decomposed into equally strong  $\sigma_+$  and  $\sigma_-$  components, driving Raman transitions between magnetic sublevels ( $\Delta m = 2$ ). In the presence of a magnetic field along the  $x$ -direction, the above description remains valid after transformation to a frame co-rotating with the Larmor frequency  $\omega_L$ . Consequently, the frequencies of the two Raman fields have to be shifted by  $\pm\omega_L$  to meet the two-photon resonance condition (see Fig. 1(b)). In this sense, spin squeezing corresponds to the creation of paired excitations of the spin at frequency  $2\omega_L$  and will reveal itself in the Fourier component of the rotating spin at frequency  $\omega_L$ .

Naturally, this type of interaction is non-linear only in spin components of individual atoms. Therefore, the maximally possible degree of squeezing [7] is limited by the total spin of a single atom, while the total spin of an

ensemble can be arbitrarily high. With one-axis twisting, the squeezing is further limited by the deviation of the resulting QPD from a geodesic in the spherical phase space. This finding is equivalent to the differential light shift imposed on magnetic sublevels in the  $x$ -basis, which inevitably accompanies the Raman coupling and detunes the coupling between different sublevels. A somewhat higher degree of squeezing can be achieved with a two-axis countertwisting Hamiltonian of the form  $H_s = \alpha(\hat{F}_z^2 - \hat{F}_y^2)$ [21]. Taking the decreasing mean spin into account, squeezing parameters of  $\chi^2 \approx 0.163$ ,  $\zeta^2 \approx 0.247$ , and  $\xi^2 \approx 0.327$  can be reached with this Hamiltonian, using the maximum available spin of  $F = 4$  in ground state Cesium atoms. The required Hamiltonian could, e.g., be implemented with two laser fields of orthogonal polarizations (along rotating  $y'$ - and  $z'$ -directions) and opposite detunings from an atomic resonance. Here, we balance the light shift instead with the second-order Zeeman shift  $\hat{H}_Z = \beta \hat{F}_x^2$ , such that all energy splittings between magnetic substates of the  $F = 4$ -manifold coincide. By adjusting the light intensity and detuning,  $\alpha_2 |E_z|^2 = -8\beta$  can be chosen to obtain:  $\hat{H}_s + \hat{H}_Z = -\frac{\alpha_0 |E_z|^2}{4} + \beta \hbar^2 F(F+1)/2 + \beta(\hat{F}_z^2 - \hat{F}_y^2)/2$ , using  $\hat{F}_x^2 + \hat{F}_y^2 + \hat{F}_z^2 = \hbar^2 F(F+1)$  for Eigenstates of  $\hat{\mathbf{F}}^2$ .

Coherent superpositions of magnetic sublevels similar to those described above have been recently generated by universal quantum control of a hyperfine spin in an ultra-cold ensemble [25]. In that experiment the mean values of elements of a single atom density matrix were determined. However, knowledge of the single atom density matrix is not sufficient to infer spin squeezing of the ensemble. Due to the collective preparation, the members of the ensemble will not in general be uncorrelated. Collective spin squeezing, as required for quantum limited metrology or quantum memory [8], can therefore only be determined via measurement of collective quantum fluctuations, ideally via full quantum tomography, as performed in the present paper. Only such measurements can reveal the deleterious effect of classical and quantum atom-atom correlations, which can be created in the preparation process and can easily ruin the spin squeezing of the ensemble. In particular, it is of major importance to send the driving Raman field (Fig. 1(b)) along the direction of the mean spin ( $x$ -direction). If, e.g., the orthogonal  $y$  direction is used, the quantum fluctuations of the driving field will couple via atomic  $\pi$ -transitions to the collective symmetric mode for  $\Delta m_x = 1$  coherences, and thus destroy collective spin squeezing under strong coupling conditions. In fact, this process forms the basis for quantum memory applications [9, 10].

The protocol for atomic quantum tomography used to reconstruct the collective quantum state is detailed elsewhere [10, 27, 28]. In brief, we send a strong, linearly  $y$ -polarized beam along the  $z$ -axis of the atomic ensemble, see Fig. 1(c). After the interaction, we perform po-

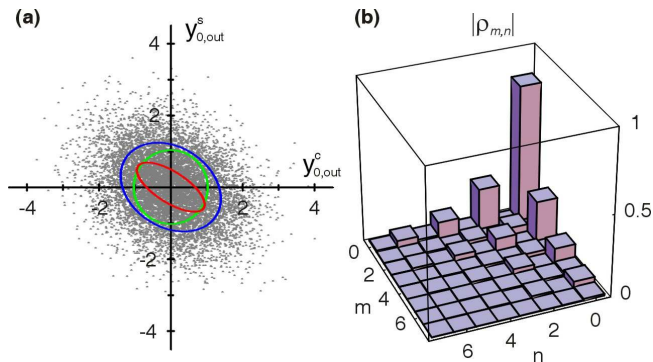


FIG. 2: Exemplified quantum state reconstruction (at  $\approx 3$  dB squeezing) with  $\kappa^2 \approx 0.8$ . (a) Scatter plot of  $10^4$  realizations. The scaled atomic covariance (red ellipse with  $\sqrt{2}\sigma$ -radii) is determined by correcting the total covariance (blue) for light and back-action noise (green). (b) Maximum likelihood estimation of the density matrix  $\hat{\rho}$  for the collective spin state, showing alternating excitation numbers  $m, n$  in the harmonic oscillator approximation. See methods section.

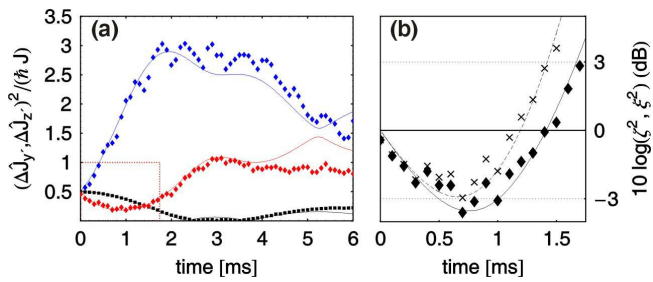


FIG. 3: (a) Results of the quantum state reconstruction for varied Raman pulse length. Red and blue diamonds show atomic squeezed ( $\equiv \chi^2/2$ ) and anti-squeezed variances, respectively. For useful squeezing, they have to be compared to the variance of a CSS with the same mean spin (black squares). (b) Resulting squeezing parameters  $\zeta^2$  (diamonds) and  $\xi^2$  (crosses), representing renormalized data from the indicated region in (a). Theoretical predictions are shown as solid and dashed lines.

larization homodyning in the  $45^\circ$ -basis, measuring the photon number difference in the two outputs, i.e. the Stokes operator  $\hat{S}_y = \hat{n}_{+45^\circ} - \hat{n}_{-45^\circ}$ . Due to the Faraday effect, the polarization of the input beam is rotated proportionally to the instantaneous atomic spin component  $\hat{J}_z$ , producing a proportional homodyne output for small rotations. The atomic spin precesses, and information on the two orthogonal, rotating spin components  $\hat{J}_{y'}$  and  $\hat{J}_{z'}$  can be obtained by evaluating the cosine and sine components of the output signal at the Larmor precession frequency  $\omega_L$ . The atomic ensemble is freshly prepared and the procedure repeated  $10^4$  times to determine the quantum statistics including the mean and variance of the collective atomic spin state.

The state tomography is illustrated in Fig. 2. Atomic variances are directly inferred from the sampled data. In addition, we performed maximum likelyhood estimations

of the collective state in the 10 best-resolved dimensions of Hilbert space [29]. The results, i.e. the measured variances, are shown in Fig. 3 together with predictions from a density matrix calculation. Our model includes atomic decay due to spontaneous emission and incorporates independently measured values for depolarizing and dephasing times in the dark ( $T_1 = 80$  ms,  $T_2 = 20$  ms). We kept the effective light power in the cell as a free model parameter, but especially for short times, the theoretical results are stable against small variations in the control parameters. The used light power slightly overcompensates the second-order Zeeman-shift, and our model suggests better performance at even higher powers as it identifies atomic decay as the dominant limitation. We consistently achieve squeezing of a canonical variable by  $\zeta^2 = 0.47 \pm 0.1$ . Quantum memory [9] and metrology applications gain by  $\xi^2 = 0.54 \pm 0.1$ .

In conclusion, we demonstrated unconditional squeezing of a collective spin with a noise reduction of  $\approx -3$  dB by generation of entanglement within individual members of the ensemble. We have fully characterized the non-classical collective atomic state via quantum state tomography. The method developed in this paper is independent and complementary to the ensemble entanglement and squeezing approach based on quantum-non-demolition (QND) measurements [8, 12, 13]. Indeed it can, e.g., be directly applied, either separately or in combination with the QND method, to enhance the fidelity of the quantum memory [9]. It may also find use in spectroscopic applications, such as magnetometry beyond the SQL.

## METHODS

### State preparation

In our experiment, we employ a room temperature ensemble of  $N \approx 10^{12}$   $^{133}\text{Cs}$  atoms, contained in a paraffin coated,  $22 \times 22 \times 22$  mm<sup>3</sup> glass cell. The cell is shielded against field fluctuations and subjected to a homogeneous magnetic field along the  $x$ -direction of  $B_x \approx 0.9$  G. By fine-tuning the magnetic field we adjust the atomic Larmor precession to a reference frame rotating at  $\omega_L = 2\pi \times 322$  kHz, which is defined by a computer controlled radio frequency (rf) synthesizer.

The experimental pulse sequence consists of three stages and is depicted in Fig. 1. The two-step state preparation starts with an 8 ms long optical pump pulse of two resonant, circularly polarized beams, propagating along the  $x$ -direction. See Fig. 1(a). After optical pumping, we find 98% of the atoms in the  $|F = 4, m_x = 4\rangle$  state, by evaluating the magneto-optical resonance signal (MORS) [26]. At the second stage, we coherently transfer atomic population between even magnetic sub-states of the  $F = 4$ -manifold by driving Raman transi-

tions on the  $D_1$ -line for a variable duration  $T_R = 0-6$  ms with a single photon detuning of  $\Delta_R = -550$  MHz from the  $6^2S_{1/2}, F = 4 \rightarrow 6^2P_{1/2}, F' = 4$  transition. See Fig. 1(b). The two-photon difference  $\nu_R \approx 644.2$  kHz is resonant with the  $m_x = 4 \rightarrow m_x = 2$  transition, including corrections for second-order Zeeman and differential light shifts. Finally, the collective atomic state is analyzed via off-resonant Faraday interaction with a strong ( $P \approx 5$  mW), linearly polarized, 2 ms long probe pulse. The probe laser frequency is close to the  $D_2$ -line with a blue-detuning of  $\Delta_P = 825$  MHz from the  $F = 4 \rightarrow F' = 5$  transition. See Fig. 1(c).

Some experimental issues have to be considered for the generation of collective squeezed states. The state preparation must be completed on a timescale short compared to decoherence mechanisms, e.g. caused by inhomogeneous fields, atom-atom, and atom-wall collisions. Therefore, the strength of the squeezing interaction should be maximized. Although atomic motion leads to averaging, it is necessary, particularly on short time scales, to provide rather homogeneous coupling strength over the cell volume with expanded, mode-matched Raman fields. A small angle between the two beams leads to a varying relative phase over the cell volume, which gives rise to a residual Doppler shift for moving atoms and results in incoherent squeezing. A similar effect is caused by the collective spin of the polarized ensemble. Due to the Faraday-effect, the sample is circularly birefringent and induces a phase shift over the cell length,  $\Delta\phi < 12^\circ$  for our parameters. A simple and robust experimental approach is to generate the necessary Raman fields by amplitude modulation of a single, linearly polarized light beam. But to avoid the additional sidebands and minimize spontaneous emission, we mode-match two phase-stable, circularly polarized fields. For ground state alkali atoms, the tensor polarizability compared to the scattering rate is limited by the excited state hyperfine splitting. Their ratio is optimal when tuned between the hyperfine transitions of the  $D_1$  line, ( $F = 4 \rightarrow F' = 3, 4$ ) at 894 nm for Cesium. At this detuning, the tensor polarizability is also largest and stationary and thus independent of atomic velocity. In addition, it has the correct sign for compensation of the second-order Zeeman shift.

### State reconstruction

The commutation relation prevents us from measuring both spin components with arbitrary precision, and their precise values are masked by back-action of the original light noise. Their statistical moments, however, can be inferred from the moments of the light output. For large atom numbers, we can make a harmonic oscillator approximation and define canonical operators as  $\hat{x} = \hat{J}_{y'}/\sqrt{\hbar\langle\hat{J}_x\rangle}$ ,  $\hat{p} = \hat{J}_{z'}/\sqrt{\hbar\langle\hat{J}_x\rangle}$  for atomic variables

and  $\hat{y} = \hat{S}_y/\sqrt{\langle\hat{S}_x\rangle}$ ,  $\hat{q} = \hat{S}_z/\sqrt{\langle\hat{S}_x\rangle}$  for light variables of a given mode with  $[\hat{x}, \hat{p}] \approx [\hat{y}, \hat{q}] \approx i$ . The two simultaneously accessible output variances are given by:

$$(\Delta\hat{y}_{0,\text{out}}^{\text{c,s}})^2 = (\Delta\hat{y}_0^{\text{c,s}})^2 + \frac{\kappa^2}{2}(\Delta\hat{x}, \Delta\hat{p})^2 + \frac{\kappa^4}{12}(\Delta\hat{q}_1^{\text{s,c}})^2, \quad (2)$$

where the indices correspond to different, non-orthogonal temporal modes of the light field, oscillating as cosine (c) and sine (s) components at the Larmor frequency. Index 0 refers to a rectangular envelope of duration  $T$ , and  $\kappa^2 \propto J_x T$ .

We scale the time-integrated homodyne output by referencing it to the light vacuum noise,  $\langle(\Delta\hat{y})^2\rangle = \langle(\Delta\hat{q})^2\rangle = 1/2$ . To avoid changes in the optical and electronic paths, this is measured by shifting the atomic Larmor frequency well outside the detection bandwidth using the magnetic field. The coupling strength  $\kappa^2$  is calibrated by measuring the resonant noise of the atomic ensemble in thermal equilibrium. For the thermal state, the back-action noise is zero and the output noise is given by the light noise and the atomic contributions from thermally populated states in the  $F = 4$ -manifold:  $(\Delta\hat{y}_{0,\text{out}}^{\text{c,s}})^2 = \frac{1}{2} + \frac{\kappa^2}{2\hbar J_x}(\Delta\hat{J}_{y',z'})^2 = \frac{1}{2} + \frac{\kappa^2 N \hbar}{2 J_x} \cdot \frac{15}{16}$ . In principle, the second-order Zeeman-shift of the magnetic sub-levels has to be considered, but it is compensated by the differential light shift induced by the probe laser. The measurement of the mean spin  $J_x/N$  is calibrated with a fully pumped ensemble.

The density matrix for the collective spin state is represented in a basis given by excitation operators defined as  $b, b^\dagger = (\hat{x} \pm i\hat{p})/\sqrt{2}$  and  $\hat{m}, \hat{n} = b^\dagger b$ . See Fig. 2.

### ACKNOWLEDGEMENTS

We thank J. H. Müller and M. Christandl for helpful discussions. This work was supported by the EU under contracts FP6-015848 (QAP) and FP6-511004 (COVAQUIAL).

\* Present address: Institut für Physik, Johannes-Gutenberg Universität, D-55099 Mainz, Germany

† Electronic address: polzik@nbi.dk

- [1] Kitagawa M., Ueda, M. Nonlinear-Interferometric Generation of Number-Phase-Correlated Fermion States. Phys. Rev. Lett. **67**, 1852-1854 (1991).
- [2] Leibfried, D. et al. Towards Heisenberg-Limited Spectroscopy with Multiparticle Entangle States. Science **304**, 1476-1478 (2004).
- [3] Geremia, J. M., Stockton, J. K., Mabuchi, H. Suppression of Spin Projection Noise in Broadband Atomic Magnetometry. Phys. Rev. Lett. **94**, 203002 (2005).
- [4] Petersen, V., Madsen, L. B., Mølmer, K. Magnetometry with entangled atomic samples. Phys. Rev. A **71**, 012312 (2005).

- [5] Roos, C. F., Chwalla, M., Kim, K., Riebe, M., Blatt, R. 'Designer atoms' for quantum metrology. *Nature* **443**, 316-319 (2006).
- [6] Windpassinger, P. J. et al. Non-Destructive Probing of Rabi Oscillations on the Cesium Clock Transition near the Standard Quantum Limit. arXiv:0801.4126[quant-ph].
- [7] Sørensen, A. S., Mølmer, K. Entanglement and Extreme Spin Squeezing. *Phys. Rev. Lett.* **86**, 4431-4434 (2001).
- [8] Julsgaard, B., Kozhekin, A., Polzik, E. S. Experimental long-lived entanglement of two macroscopic objects. *Nature* **413**, 400-403 (2001).
- [9] Julsgaard, B., Sherson, J., Cirac, J. I., Fiurášek, J., Polzik, E. S. Experimental demonstration of quantum memory for light. *Nature* **432**, 482-486 (2004).
- [10] Sherson, J. F. et al. Quantum teleportation between light and matter. *Nature* **443**, 557-560 (2006).
- [11] Hald, J., Sørensen, J. L., Schori, C., Polzik, E. S. Spin Squeezed Atoms: A Macroscopic Entangled Ensemble Created by Light. *Phys. Rev. Lett.* **83**, 1319-1322 (1999).
- [12] Kuzmich, A., Mandel, L., Bigelow, N. P. Generation of Spin Squeezing via Continuous Quantum Nondemolition Measurement. *Phys. Rev. Lett.* **85**, 1594-1597 (2000).
- [13] Geremia, J. M., Stockton, J. K., Mabuchi, H. Real-Time Quantum Feedback Control of Atomic Spin-Squeezing. *Science* **304**, 270-273 (2004).
- [14] Duan, L.-M., Lukin, M. D., Cirac, J. I., Zoller, P. Long-distance quantum communication with atomic ensembles and linear optics. *Nature* **414**, 413-418 (2001).
- [15] Matsukevich, D. et al. Entanglement of remote atomic qubits. *Phys. Rev. Lett.* **96**, 030405 (2006).
- [16] Chou, C.-W. et al. Functional Quantum Nodes for Entanglement Distribution over Scalable Quantum Networks. *Science* **316**, 1316-1320 (2007).
- [17] Chen S. et al. Demonstration of a Stable Atom-Photon Entanglement Source for Quantum Repeaters. *Phys. Rev. Lett.* **99**, 180505 (2007).
- [18] Simon J., Tanji, H., Thomson, J. K., Vuletić, V. Interfacing Collective Atomic Excitations and Single Photons. *Phys. Rev. Lett.* **98**, 183601 (2007).
- [19] Honda, K. et al. Storage and Retrieval of a Squeezed Vacuum. arXiv:0709.1785[quant-ph].
- [20] Appel, J., Figueroa, E., Korystov, D., Lvovsky A. I. Quantum memory for squeezed light. arXiv:0709.2258[quant-ph].
- [21] Kitagawa, M., Ueda, M. Squeezed spin states. *Phys. Rev. A* **47**, 5138-5143 (1993).
- [22] Wineland, D. J., Bollinger, J. J., Itano, W. M., Moore, F. L., Heinzen, D. J. Spin squeezing and reduced quantum noise in spectroscopy. *Phys. Rev. A* **46**, R6797-R6800 (1992).
- [23] Wineland, D. J., Bollinger, J. J., Itano, W. M., Heinzen, D. J. Squeezed atomic states and projection noise in spectroscopy. *Phys. Rev. A* **50**, 67-88 (1994).
- [24] Sørensen, A., Duan, L.-M., Cirac, J. I., Zoller, P. Many-particle entanglement with Bose-Einstein condensates. *Nature* **409**, 63-66 (2001).
- [25] Chaudury, S. et al. Quantum Control of the Hyperfine Spin of a Cs Atom Ensemble. *Phys. Rev. Lett.* **99**, 163002 (2007).
- [26] Julsgaard, B., Sherson, J., Sørensen, J. L., Polzik, E. S. Characterizing the spin state of an atomic ensemble using the magneto-optical resonance method. *J. Opt. B: Quantum Semiclass. Opt.* **6**, 5-14 (2004).
- [27] Usami, K., Takahashi, J.-i., Kozuma, M. How to measure the quantum state of collective atomic spin excitation. *Phys. Rev. A* **74**, 043815 (2006).
- [28] Sherson, J., Julsgaard, B., Polzik, E. S. Deterministic atom-light quantum interface. *Adv. At. Mol. Opt. Phys.* **54**, 81-130 (2006).
- [29] Hradil, Z., Mogilevtsev, D., Řeháček, J. Biased Tomography Schemes: An Objective Approach. *Phys. Rev. Lett.* **96**, 230401 (2006).